

In-Depth Comparison of Matrigel Dissolving Methods on Proteomic Profiling of Organoids

Authors

Man Wang, Huan Yu, Ting Zhang, Lihua Cao, Yang Du, Yuhao Xie, Jiafu Ji, and Jianmin Wu

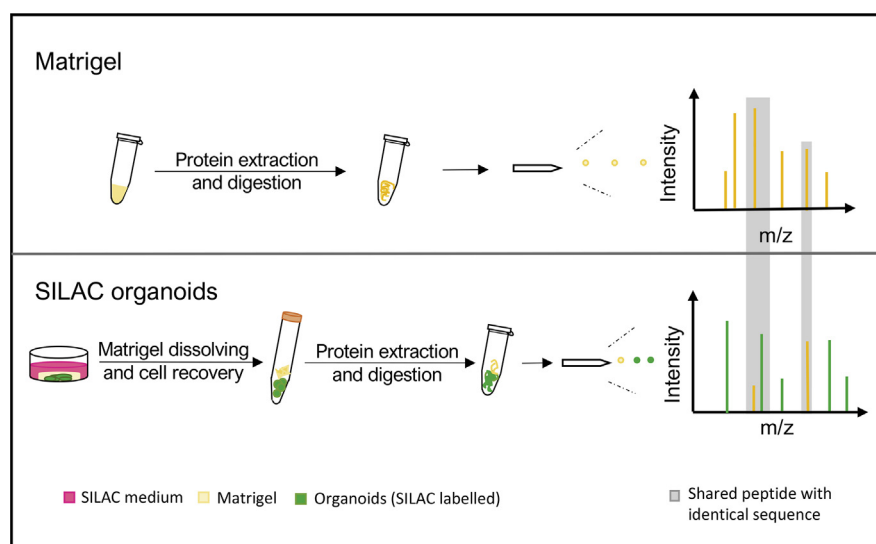
Correspondence

wujm@bjmu.edu.cn

Graphical Abstract

In Brief

Matrigel has a complex composition, and insufficient separation of organoids from Matrigel could influence proteomic profiling of organoids significantly. Here, we performed an in-depth quantitative comparison of three Matrigel dissolving methods, and dispase was identified as a satisfying method in multiple ways. A list of high-confidence Matrigel contaminants was also identified, to help eliminate interference of undissolved Matrigel in proteomic analysis of organoids, collected by cell recovery solution or PBS-EDTA buffer.



Highlights

- A comprehensive comparison of Matrigel dissolving methods on organoid proteomics.
- Matrigel leftover influences protein identification and quantification for organoids.
- Dispase is a satisfying method for proteomic sample preparation of organoids.
- Exclusion of high-confidence Matrigel contaminants attenuates Matrigel interference.

In-Depth Comparison of Matrigel Dissolving Methods on Proteomic Profiling of Organoids

Man Wang^{1,‡}, Huan Yu^{1,‡}, Ting Zhang¹, Lihua Cao¹, Yang Du¹, Yuhao Xie², Jiafu Ji³, and Jianmin Wu^{1,4,*}

Patient-derived organoids recently emerged as promising *ex vivo* 3D culture models recapitulating histological and molecular characteristics of original tissues, thus proteomic profiling of organoids could be valuable for function investigation and clinical translation. However, organoids are usually cultured in murine Matrigel (served as scaffolds and matrix), which brings an issue to separate organoids from Matrigel. Because of the complex compositions of Matrigel and thousands of identical peptides shared between Matrigel and organoids, insufficiently dissolved Matrigel could influence proteomic analysis of organoids in multiple ways. Thus, how to dissolve Matrigel matrix and recovery organoid cells efficiently is vital for sample preparation. Here, we comprehensively compared three popular Matrigel dissolving methods (cell recovery solution, dispase, and PBS–EDTA buffer) and investigated the effect of undissolved Matrigel proteins on proteomic profiles of organoids. By integrative analysis of label-free proteomes of Matrigel and stable isotope labeling by amino acids in cell culture proteomes of organoids collected by three methods, respectively, we found that dispase showed an optimal efficiency, with the highest peptide yield and the highest incorporation ratio of stable isotope labeling by amino acids in cell culture labels (97.1%), as well as with the least potential Matrigel contaminants. To help analysis of proteomic profiles of organoids collected by the other two methods, we identified 312 high-confidence Matrigel contaminants, which could be filtered out to attenuate Matrigel interference with minimal loss of biological information. Together, our study identifies bioinformatics and experimental approaches to eliminate interference of Matrigel contaminants efficiently, which will be valuable for basic and translational proteomic research using organoid models.

The advent of new 3D cell culture systems, known as organoid culture, has shown the promising potentials in biomedical research, as organoids could recapitulate

histological and molecular characteristics of original tissues (1–5). Therefore, compared with classical 2D cell cultures, proteomic profiles of organoids were thought to have better relevance with clinical features and patient outcomes (6–8), which could be valuable for biomarker discovery and function verification.

Most organoid culturing systems rely on basement-membrane matrix (known as basement-membrane extract/Matrigel) extracted from Engelbreth–Holm–Swarm mouse sarcomas, serving as scaffolds and matrix mimicking extracellular matrix (ECM) (4, 9–11). It raises a special process of Matrigel dissolving for cell recovery (CR) and protein extraction for organoid proteomics analysis. Although ECM proteins (such as laminin, collagen IV, and entactin) constitute the bulk of Matrigel, there are more than 1800 proteins identified in Matrigel including numerous intracellular proteins involved in metabolic pathways and other important biological processes (12). Because of this complex composition of Matrigel and thousands of identical peptides shared between Matrigel and organoids, the efficiency of Matrigel dissolving would influence proteomic analysis of organoids in multiple perspectives. First, high abundances of undissolved Matrigel proteins (“Matrigel contaminants”) would waste numerous mass spectrum scans, which could result in less identification of organoid proteins. Second, organoid proteins might be misidentified because of the identical peptides from Matrigel contaminants. Besides, abundances of organoid proteins uniquely represented by these shared peptides could be estimated with a bias, including a misincrease in label-free and isobaric tags for relative and absolute quantification or tandem mass tags–labeled proteomic analysis, and a misdecrease of incorporation degrees in metabolic-labeled proteomic analysis.

Different approaches have been applied to isolate organoids from Matrigel, in which nonenzymatic dissociation using

From the ¹Key Laboratory of Carcinogenesis and Translational Research (Ministry of Education/Beijing), Center for Cancer Bioinformatics, Peking University Cancer Hospital and Institute, Beijing, China; ²Institute of Systems Biomedicine, School of Basic Medical Sciences, Peking University Health Science Center, Beijing, China; ³Key Laboratory of Carcinogenesis and Translational Research (Ministry of Education/Beijing), Gastrointestinal Cancer Center, Peking University Cancer Hospital and Institute, Beijing, China; ⁴Peking University International Cancer Institute, Peking University, Beijing, China

[‡]These authors contributed equally to this work.

*For correspondence: Jianmin Wu, wujm@bjmu.edu.cn.

CR solution (also named “Matrisperse” previously) (2, 13–15), enzymatic digestion using dispase (3, 16–18), and chemical method involving PBS–EDTA (PE) buffer are widely used (8, 9, 19). However, differences in Matrigel dissolving efficiency between these methods and the corresponding effect are unknown. Several studies considered the aforementioned issues by blacklisting all proteins identified in Matrigel for proteomic analysis of mouse-derived organoids (20) or removing corresponding human homologous proteins for proteomic analysis of human organoids (21), before downstream analysis to avoid the potential interference. But these filtering strategies have not considered relative abundances of shared peptides contributed by organoids and Matrigel contaminants, respectively. Moreover, although a substantial proportion of shared peptides of functional proteins had high abundances in organoids and low abundances in Matrigel, they could be filtered out unintendedly by these strategies. Thus, it will be valuable to systematically investigate the differences between different Matrigel dissolving methods and exactly evaluate their influences on organoid proteomic profiles. Moreover, it is warranted to generate a high-confidence list of Matrigel contaminants for precise filtering, which may save numerous potential human biomarker proteins from the previous filtering strategy.

In this study, we performed comprehensive MS-based proteomic analyses of patient-derived tumor organoids and Matrigel to compare the influences of three popular Matrigel dissolving methods on proteomic profiling of organoids, as well as, to identify high-confidence Matrigel contaminants (hCMCs) to help eliminate undissolved Matrigel interference with minimal loss of biological information.

EXPERIMENTAL PROCEDURES

Organoid Culture

Gastric cancer tissue was obtained from The Peking University Cancer Hospital, and the study was approved by Peking University Cancer Hospital Review Board (protocol number: 2019KT111) in accordance with the Declaration of Helsinki. Gastric cancer organoids were established and cultured as previously reported (22). Briefly, established organoids were embedded in Matrigel (Corning; catalog no.: 356231) with addition of organoid culture medium, including advanced Dulbecco's modified Eagle's medium (DMEM)/F12, 1% penicillin/streptomycin (Invitrogen), 1× Gluta Max (Invitrogen), 1× HEPES (Invitrogen), 1× B27 (Invitrogen), 10 mM *N*-acetylcysteine (Sigma), 50 mg/ml nicotinamide (Sigma), 500 ng/ml FGF10 (PeproTech, Inc), 500 ng/ml Noggin (PeproTech, Inc), 500 ng/ml R-spondin-1 (PeproTech, Inc), 2 μM A-8301 (Tocris), 100 ng/ml Wnt3a (R&D Systems), 10 μM Y-27632 (Sigma), epidermal growth factor (Invitrogen), gastrin (Tocris), and primocin (0.1 mg/ml; Invitrogen). Fresh medium was changed every 2 to 3 days. Organoids were split every 5 to 7 days in a 1:3 ratio using mechanical dissociation and plated in fresh Matrigel.

Stable Isotope Labeling by Amino Acids in Cell Culture

For the stable isotope labeling by amino acids in cell culture (SILAC)-based quantitative MS analysis, organoids were cultured in

the medium (“heavy”) with advanced DMEM/F-12 replaced by SILAC advanced DMEM/F-12 medium (Gibco). L-Arginine (13C6) hydrochloride (Sigma) and L-lysine (13C6, 15N2) hydrochloride (Sigma) were added in SILAC heavy medium at a working concentration of 86.4 and 152.3 mg/l, respectively. Organoids were maintained in SILAC heavy medium for several passages to allow SILAC isotope incorporation. Samples were collected after 28 days and cultured and analyzed by MS to estimate incorporation by heavy/light ratios.

Matrigel Dissolving by Dispase

Before CR, supernatant medium was discarded, and organoids covered in Matrigel were collected using PBS. Samples were then washed twice with PBS. In order to recover cells using dispase solution, 5 U/ml dispase (Stemcell) was diluted to 1 U/ml by basal SILAC advanced DMEM/F-12 medium. Diluted and prewarmed dispase solution was added (1 ml/well) in washed samples for incubation at 37 °C. After incubation for 30 min, centrifugation was done to remove the supernatant, and fresh dispase solution (1 ml/well) was added for another incubation at 37 °C for 30 min. Organoid cells were then pelleted and washed twice using PBS before cell lysis.

Matrigel Dissolving by PE Buffer

Preparation and application of PE buffer referenced the previously published protocol (9). For every milliliter of PE buffer, 100 μl of 10× protease-phosphatase stock, 20 μl of 500 mM EDTA, and 880 μl of Dulbecco's PBS were combined. It was prepared fresh before every use. Organoids were collected and washed by PBS as described for dispase method. For every 100 μl of Matrigel, 2 ml of PE buffer was added and incubated for 30 min at 4 °C. Then, centrifugation was carried out to discard the supernatant, and fresh PE buffer was added for another incubation at 4 °C for 30 min. Organoid cells were then pelleted and washed twice using PBS before cell lysis.

Matrigel Dissolving by CR Solution

Before Matrigel dissolving, organoids were also collected and washed by PBS, and then 2 ml of CR solution (the composition of the solution has not been disclosed by the vendor, Corning) was added to each well for incubation at 4 °C for 30 min. Then, centrifugation was carried out to discard the solution, and fresh CR solution was added for another incubation at 4 °C for 30 min. Organoid cells were then pelleted and washed twice using PBS before cell lysis.

Pressure Cycling Technology–Assisted Preparation of Organoid Samples

As the early passages of patient-derived tumor organoids could provide only a limited amount of cells for multiple experiments, including protein extraction, DNA/RNA extraction, and drug screening, we chose pressure cycling technology (PCT), a rapid and an efficient protein extraction procedure that is suitable for precious clinical samples (23). After CR, the PCT-assisted lysis and digestion were processed based on the reported protocol. Briefly, 30 μl of lysis buffer was added into the microtube, which contains 6 M urea, 2 M thiourea, and 0.1 M ammonium bicarbonate. And the organoids were lysed using PCT-micropestle in a barocycler HUB440 (Pressure Bio-Sciences, Inc). Then the extracted proteins were reduced and alkylated by incubating simultaneously with Tris(2-carboxyethyl) phosphine and iodoacetamide. Afterward, lysC (1:40) and trypsin (1:50) digestion were performed in the barocycler with digestion program. Then the peptides were acidified with 10% trifluoroacetic acid to pH 2 to 3 and desalted with Sep-Pak C18 cartridges (Waters). Before MS analysis, the peptides were dissolved with MS buffer, which contains 0.1% formic acid and 2% acetonitrile in HPLC-grade

water. And the peptide concentration was measured with NanoDrop One (Thermo Fisher Scientific).

Precipitation and Digestion of Matrigel Proteins

As PCT is not suitable for samples with bigger volume limited by the microtube, we chose cold acetone to precipitate the Matrigel proteins at -20°C overnight. About 500 μl of cold acetone was added into 100 μl Matrigel and incubated for overnight at -20°C . After centrifugation, the protein pellet was resuspended in 8 M urea buffer and subjected to reduction and alkylation. Then the proteins were digested in solution, and subsequently, the tryptic peptides were desalted with Sep-Pak C18 cartridges (Waters).

Analytical Methods

All samples were analyzed using a Q Exactive HF-X Orbitrap mass spectrometer (MS) coupled with an EASY nLC 1200 system (Thermo Fisher Scientific). The peptides were loaded onto a home-made reversed-phase analytical column (1.9 μm , length of 25 cm, and 100 μm i.d.) for separation. Solvent A was 0.1% formic acid/2% acetonitrile/98% water, and solvent B was 0.1% formic acid/90% acetonitrile/10% water. A 120 min (90 min for Matrigel peptides) gradient from 3% to 30% solvent B at 550 nl/min was used for the separation. Full MS scans were acquired for the mass range of 400 to 1200 m/z at the resolution of 60,000. Top 20 abundant ions were fragmented by data-dependent MS/MS experiments with an isolation window of 1.6 m/z , the exclusion duration of 30 s, and at a normalized collision energy of 32% for higher-energy collisional dissociation. The charge state of 1 was discarded. The MS/MS scans were acquired at a resolution of 15,000 with a fixed first m/z of 120 m/z . Maximum injection time was 60 and 100 ms for full MS and MS/MS scan, respectively. The automatic gain control target value was set to 5×10^4 and 1.0×10^4 for full MS and MS/MS scans, respectively.

Raw Data Processing and Database Search

Raw MS files of organoid samples were searched using MaxQuant (version 1.6.14.0) against SwissProt *Homo sapiens* database (February 2018; 20,269 entries) (24). The defined fixed modification was carbamidomethylation of cysteines, whereas methionine oxidations and protein N-terminal acetylations were set as variable modifications. The peptide tolerance for main search was 10 ppm, and the MS/MS match tolerance was 20 ppm. Two missed cleavages were allowed for enzymatic cleavage with trypsin/P. The option “match between runs” was also enabled. Quantitation was performed with a setting of label free (for label-free experiments) or double SILAC (for SILAC experiments). The final list of peptides was obtained after applying a 1% false discovery rate. For proteins, only proteins with at least one unique peptide were considered. Nonunique peptides were assigned to corresponding proteins, according to the Razor peptides rule implemented in MaxQuant. Finally, the identified peptides and proteins were filtered to remove peptides/proteins tagged as “REV” and “CON.” For Matrigel samples, database search was against SwissProt mouse database (January 2020; 17,027 entries), and quantitation was performed using MaxQuant label-free mode. Other parameters were same as analysis of organoid samples.

Experimental Design and Statistical Rationale

To keep the same condition for comparison, we used the same passage of organoids established from one patient. Three biological replicates were set for each organoid proteomic experiment. For the comparison of three Matrigel dissolving methods, the same batch of SILAC heavy-labeled organoids was used, and the same number of wells was collected for each method. For the Matrigel proteomic

experiment, three batches of Matrigel (lot nos. 0055015, 0223001, and 0232003) were prepared simultaneously, and two replicates were set for each batch.

Results were visualized using violin plot, bubble plots, box plots, and volcano plots, using R package *ggplot2*. Histograms and scatter diagrams were plotted by Microsoft Excel. Venn diagrams were generated by VENNY2.1 (<https://bioinfo.cnb.csic.es/tools/venny/index.html>).

RESULTS

Comparison of Three Matrigel Dissolving Methods

First, we evaluated the performance of CR solution, dispase, and PE buffer regarding CR and protein extraction. The yield of peptides extracted in dispase group was more than twice of yields in CR/PE groups, using the same number of wells of organoid collected as input (Fig. 1A, $p < 0.01$). This could be due to the mild nature of CR and PE, leading to insufficient separation of Matrigel and organoid cells, with a portion of cells discarded with Matrigel in supernatant after centrifugation. This was consistent with experimental observation during Matrigel dissolving process, for example, Matrigel was removed faster by dispase, and bigger volume of cell pellets was collected in dispase than the other two groups (Fig. 1B).

To precisely distinguish Matrigel proteins from organoid proteomes, we labeled organoid proteins with SILAC. Heavy lysine and arginine were added in SILAC medium, and organoid proteins were labeled by metabolic incorporation of heavy amino acids (“heavy”), whereas Matrigel proteins kept natural state (“light”). After MS analysis and database search, the greatest number of peptides and proteins was identified in dispase group (Fig. 1, C and D), implying more waste of MS scans by Matrigel contaminants in CR/PE groups. Furthermore, the highest incorporation ratio of heavy amino acids was also achieved in dispase group (>97%), which was significantly higher than the other two groups (Fig. 1E, $p < 0.01$). Together, these results suggested that more Matrigel proteins might be retained in the CR and PE groups, resulting in lower incorporation ratios and less identified peptides and proteins.

To further investigate the effect of undissolved Matrigel contaminants, we performed label-free proteomic analysis of three batches of Matrigel, as Matrigel has been reported with batch-to-batch variation (25). As a result, 3677 identical peptides in total were identified to be shared between murine Matrigel and human organoid proteomic profiles, corresponding to 927 Matrigel proteins, termed as potential Matrigel contaminants (pMCs) (supplemental Fig. S1 and supplemental Table S1). Next, we screened out the shared peptides with low incorporation ratios (<97%, termed as LIR-M peptides) in SILAC organoid profiles for each group, and dispase group showed the least LIR-M peptides and proteins as expected (Fig. 2A and Table 1). The differences were more striking regarding the identical peptides that were

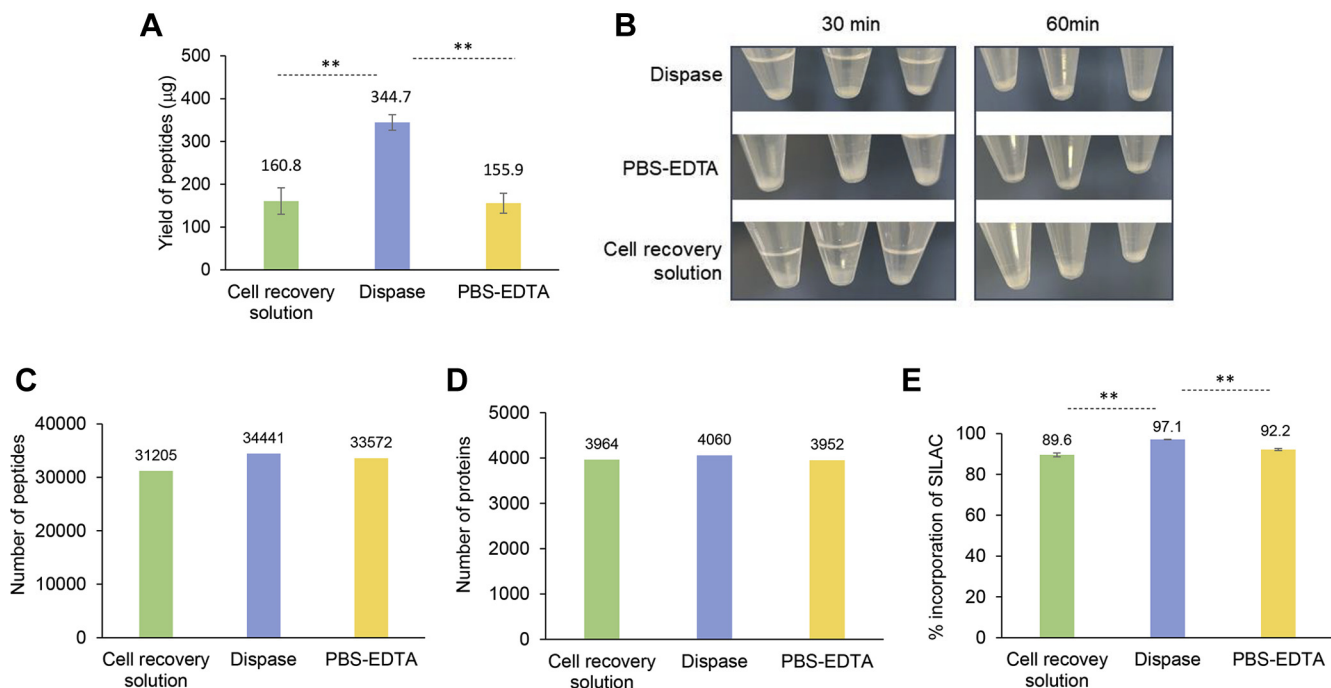


FIG. 1. Overview of differences between three Matrigel dissolving methods. *A*, bar plots presenting yields of peptides for samples collected by different methods (** indicates $p < 0.01$, t test). *B*, photos of cell pellets collected after incubation (30 and 60 min) using three Matrigel dissolving methods, illustrating diverse Matrigel removing efficiencies. More Matrigel and less cells were observed in PBS-EDTA and cell recovery solution groups. *C* and *D*, number of peptides (*C*) and proteins (*D*) identified in SILAC-labeled organoids collected by three methods. *E*, the respective incorporation ratios of SILAC amino acids in organoid proteomic profiles collected by three methods, with each triplicate method. SILAC, stable isotope labeling by amino acids in cell culture.

shared between organoid peptides with zero incorporation ratio (ZIR) and Matrigel proteins (termed as ZIR-M peptides). Dispase group had only 15 ZIR-M peptides, whereas CR and PE groups contained 113 and 91 ZIR-M peptides, respectively (Fig. 2B and Table 1), implying that more Matrigel contaminants were misidentified as organoid

proteins in samples collected by CR or PE methods. Furthermore, we observed a higher degree of reduction in incorporation ratio difference (between total peptides and LIR-M peptides) in CR (15.3%) and PE (12.9%) groups than the dispase group (2.1%) (Table 1), which indicated a greater effect on quantitation of Matrigel contaminants in CR/PE

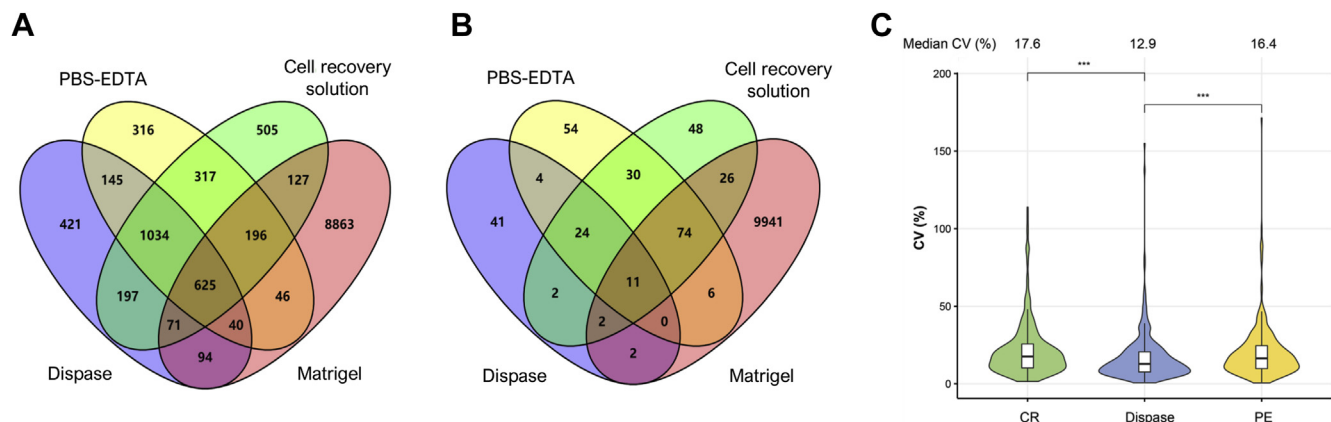


FIG. 2. Analysis of the identical peptides shared between Matrigel and organoid peptides with low ratio of SILAC incorporation. *A*, Venn diagram illustrating the relationships between Matrigel peptides (identified by label-free proteomic analysis) and organoid peptides with low SILAC incorporation ratios (<97%) collected by three methods. *B*, Venn diagram illustrating the relationships between Matrigel peptides and organoid peptides with zero SILAC incorporation ratio. *C*, Violin plot presenting the CV distributions of LIR-M protein quantification for each group (***) indicates $p < 0.001$, Wilcoxon test). LIR, low incorporation ratio; SILAC, stable isotope labeling by amino acids in cell culture.

TABLE 1
Statistics of LIR-M and ZIR-M peptides in three groups

Statistical item	CR solution		Dispase		PBS-EDTA	
	Peptides	Proteins	Peptides	Proteins	Peptides	Proteins
Number of ZIR-M peptides/proteins	113	34	15	10	91	23
Number of LIR-M peptides/proteins	1019	342	830	295	907	311
Average incorporation ratio of LIR-M peptides	74.3%		95.0%		79.3%	
Average incorporation ratio of total peptides	89.6%		97.1%		92.2%	

LIR-M, identical peptides shared between murine Matrigel and human organoid proteomes (with incorporation ratio <97%); ZIR-M, identical peptides shared between murine Matrigel and human organoid proteomes (with ZIR).

groups. Finally, we investigated reproducibility of LIR-M protein quantification, which was quantified by CV of biological triplicates. The median CV in dispase group was significantly lower than the other two groups (Fig. 2C, $p < 0.001$), which further underscored the interference of Matrigel contaminants on quantification accuracy of LIR-M proteins in CR and PE groups.

We also compared the heavy intensities of organoid proteomes between three groups to see whether different Matrigel dissolving conditions could affect protein expression, as dispase dissolved Matrigel by enzyme digestion at 37 °C, whereas the other two methods did by nonenzyme dissociation at 4 °C. Surprisingly, only few proteins showed significant difference (fold change > 2, adjusted $p < 0.05$) in the group of samples collected by dispase, compared with the other two groups (Fig. 3, A and B).

Taken together, dispase could be a decent experimental approach for proteomic studies of organoid, with the highest peptide extraction yield and satisfying Matrigel digestion efficiencies.

Development of a List of hc-MCs

To help analysis of proteomic profiles of organoids collected by CR and PE methods, we further identified a list of hc-MCs based on the LIR-M peptides that were identified in CR/PE group and unique in human proteome. As a result, 905 peptides (hc-MC peptides) were identified, corresponding to 312 murine hc-MCs. If the hc-MC peptides were removed from organoid proteomes, the incorporation ratios will be elevated to 96.1% in PE group (3.9% increase) and 95.1% in CR group (5.5% increase), demonstrating that Matrigel

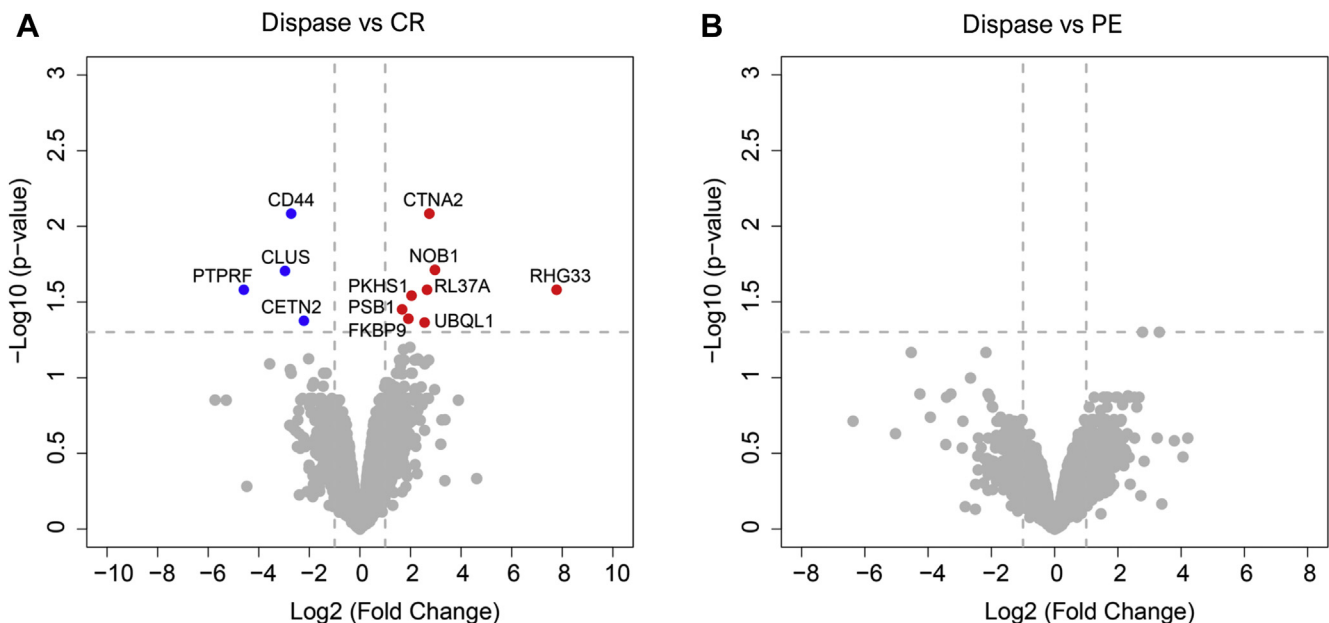


FIG. 3. Analysis of differentially expressed proteins between dispase and CR/PE group. Volcano plot depicting significance of expression difference between dispase and CR (A) or PE (B) group. A protein is considered to be significantly differentially expressed if the absolute value of log2 scaled fold change is greater than 1 (i.e., twofold change), and the adjusted p value is less than 0.05. Red dots represent significantly upregulated proteins in the dispase group, and blue dots represent significantly downregulated proteins. CR, cell recovery solution; PE, PBS-EDTA.

interference on protein quantitation could be significantly attenuated by excluding the hc-MC peptides (Fig. 4A, $p < 0.01$).

Next, we investigated the variations of hc-MCs in three batches of Matrigel. The number of identified proteins in each batch of Matrigel was similar (supplemental Fig. S2) with 78.5% of total proteins were in common among three batches (Fig. 4B), whereas 95.2% of hc-MCs were identified in all batches. Analysis of intensity-based absolute quantification, using common proteins shared between any two batches, demonstrated a highly significant correlation of protein abundances between different batches (supplemental Fig. S3; $r^2 > 0.9$). Notably, hc-MCs were identified with a higher level of abundance than the other pMCs and non-pMC proteins (Fig. 4C). In short, hc-MCs were recurrently identified in different batches of Matrigel with high abundance.

To evaluate the potential impact of 312 hc-MCs in real proteomic studies, we further investigated expression

patterns of 311 corresponding human proteins, supported by the hc-MC peptides and termed as cross-species razor proteins (CSRPs), in four published cancer proteomic datasets (26–29). Most CSRPs had significantly higher abundances than the non-CSRPs (Fig. 4D; $p < 0.001$), which highlights the need of considering the influence of hc-MC peptides in proteomic analysis of organoids. In addition, pathway analysis of CSRPs identified significant enrichment of four Kyoto Encyclopedia of Genes and Genomes pathways only (Fig. 4E, $q < 0.05$), in which amoebiasis and focal adhesion pathways were enriched because of several identified laminins, the main components of Matrigel; while enrichment of glycolysis/gluconeogenesis pathway may be due to the complex composition of Matrigel including numerous intracellular proteins identified (12). Thus, removal of 311 CSRPs from organoid proteomes may result in partial loss of biological information relevant to these pathways.

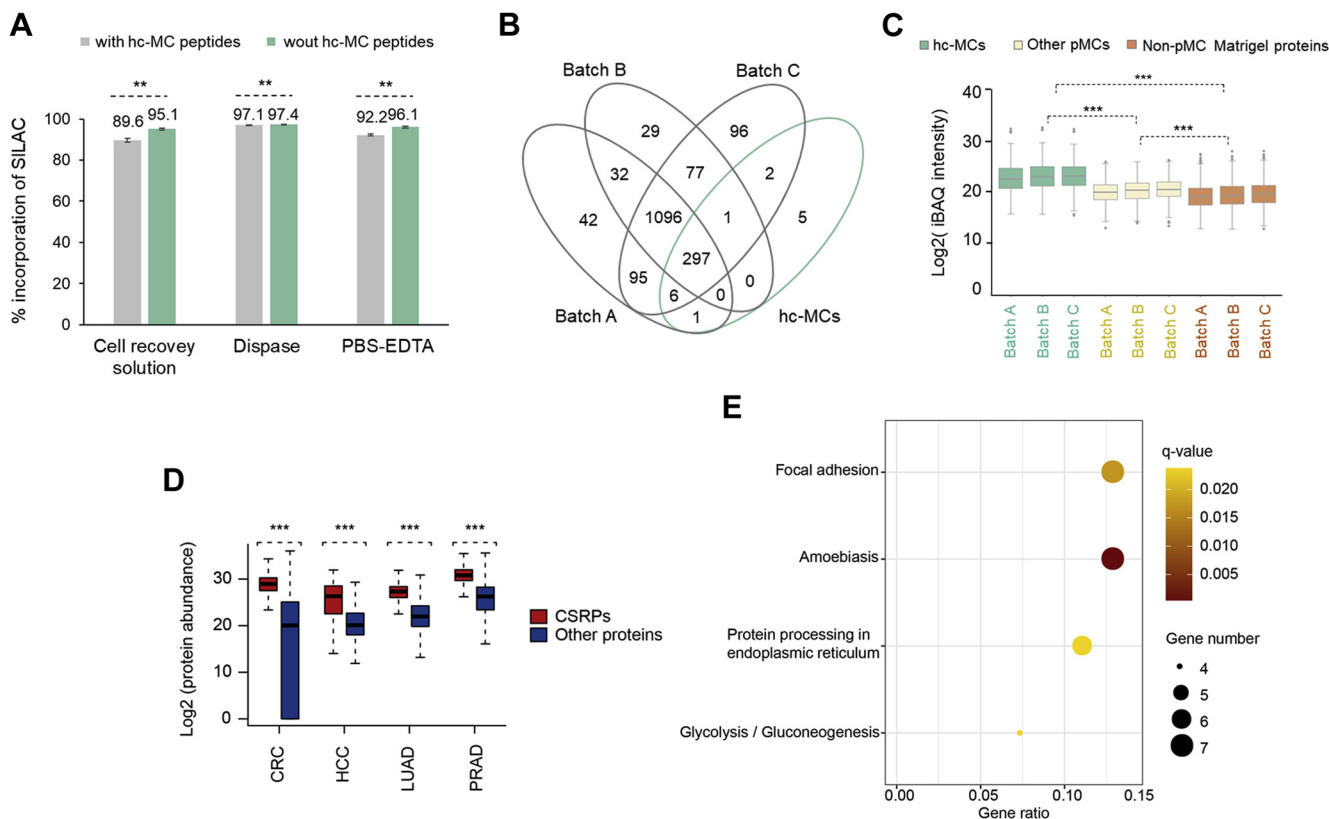


FIG. 4. **Analysis of high-confidence Matrigel contaminants.** A, grouped bar plots presenting SILAC incorporation ratios using three methods, with hc-MC peptides included and excluded (** indicates $p < 0.01$, *t* test). B, Venn diagram illustrating relationships between hc-MCs and total proteins identified in three batches of Matrigel. C, grouped bar plots showing abundance differences of hc-MCs, the remaining pMCs, and non-pMC proteins, among three batches of Matrigel (***) indicates $p < 0.001$, *t* test). D, grouped box plots showing abundance distribution of 311 CSRPs and the non-CSRP proteins, in four cancer types (CRC, HCC, LUAD, and PRAD) using published label-free proteomic datasets (***) indicates $p < 0.001$, Wilcoxon test). E, bubble plot showing enriched KEGG pathways identified in CSRPs ($q < 0.05$). Bubbles are colored according to *q* values, and size of a bubble indicates the number of identified pathway genes. CRC, colorectal cancer; CSRP, cross-species razor protein; HCC, hepatocellular carcinoma; hc-MC, high-confidence Matrigel contaminant; KEGG, Kyoto Encyclopedia of Genes and Genomes; LUAD, lung adenocarcinoma; pMC, potential Matrigel contaminant; PRAD, prostate adenocarcinoma; SILAC, stable isotope labeling by amino acids in cell culture.

DISCUSSION

Organoids have emerged as promising *ex vivo* models for personalized medicine and regenerative medicine, which are grown in a surrogate ECM (mostly Matrigel). Before the subsequent functional assay (DNA, RNA, and protein extraction), organoids must be isolated from Matrigel; thus, digesting Matrigel in an effective way is of substantial importance, because of its ill-defined composition. In this study, we comprehensively investigated the interference of insufficiently dissolved Matrigel on accurate identification and quantification of organoid proteomes and provided experimental justification for widely used Matrigel dissolving methods in the field.

Based on systematic comparison of three popular Matrigel dissolving methods, dispase showed significant advantages in sample preparation for proteomic analysis of organoids, including higher efficiencies of CR and protein extraction, more effective Matrigel elimination, more peptide identifications, and higher accuracy of quantification. Furthermore, although Matrigel contaminants exerted the influences on quantification of organoid proteins sharing identical peptides in samples collected by CR solution or PE buffer, these effects could be significantly attenuated by excluding the list of hc-MC peptides that we identified. However, there are numerous intracellular proteins existing in hc-MCs; removing all of them might result in a loss of important candidate proteins related to the biological question. Therefore, we provided the hc-MC list with peptide incorporation ratios ([supplemental Table S2](#)), for further refinements of cutoffs to accommodate diverse requirements on sensitivity depending on application scenarios.

Different with few previous filtering studies, our analysis provided deeper insights into abundance distribution of Matrigel contaminants in proteomic profiles of organoids ([supplemental Tables S3 and S4](#)), estimated by SILAC incorporation ratios, and further identified experiment and bioinformatics approaches to eliminate this interference with minimal loss of biological information irrelevant to Matrigel. This could provide more accurate identification and quantification of organoid proteins, which is the cornerstone of downstream functional analysis.

On the other hand, with the elimination of Matrigel, some organoid-specific ECM proteins would be removed inevitably at the same time. For further investigation of extracellular organoid-specific ECM proteins with a precise and an extensive coverage, it needs collection of Matrigel and medium for decellularization and enrichment of highly insoluble ECM components ([30, 31](#)). Moreover, effective methods also need to be developed for recognition of organoid-specific ECM proteins from Matrigel components.

In addition, despite the wide use of Matrigel, a number of sophisticated ECM-like scaffolds are available or in development, including collagen gel matrix and synthetic ECM

analogs ([32, 33](#)). These alternatives are generally made from collagen or synthetic gel, mainly derived from polyacrylamide and polyethylene glycol ([25](#)), with supplementation of a defined list of specific ECM proteins. Therefore, we speculate that the conclusion of Matrigel dissolving efficiencies and protein extraction yield in this study would be still useful, while the list of high-confidence containments (hc-MC for Matrigel) needs to be revised according to the specific components added in each ECM-like scaffold system.

Finally, although this study was performed using gastric cancer organoids, it could be applicable to organoids derived from other epithelial tissues (e.g., lung, mammary gland, esophagus, small intestine, colon, liver, pancreas, and prostate) and other cancer types (e.g., prostate cancer, breast cancer, liver cancer, and ovarian cancer), as Matrigel appears to be one of the essential components of this culture system, with supplementation of tissue-specific growth factors and inhibitors ([4, 11](#)).

Taken together, these findings could be helpful for proteomic and molecular research of organoid models, which is upsurging, witnessed by the recent development of “living biobank” using patient-derived organoids ([1, 15, 34–36](#)), and the advances in large-scale proteomic/proteogenomic characterization in cancer ([26–29](#)).

DATA AVAILABILITY

MS proteomics data have been deposited to the ProteomeXchange consortium (<http://proteomecentral.proteomexchange.org>) via the iProX partner repository with the dataset identifier PXD029173.

Supplemental data—This article contains [supplemental data](#).

Acknowledgments—We thank Tiannan Guo from Westlake University (Zhejiang Province, China) for instructions on PCT technology and MS analysis. This study was supported by the third round of Public Welfare Development and Reform Pilot Projects of Beijing Municipal Medical Research Institutes (Beijing Medical Research Institute, China; 2019-1), Beijing Municipal Science and Technology Commission, China (Z201100008320006), PKU-Baidu Fund, China (2019BD012), and Michigan Medicine-PKUHSC Joint Institute for Translational and Clinical Research, China (BMU2019JI010).

Author contributions—J. W. and M. W. conceptualization; M. W., H. Y., and T. Z. methodology; L. C., Y. D., and Y. X. formal analysis; M. W. investigation; J. J. resources; J. W., M. W., and H. Y. writing—original draft; J. W., M. W., and H. Y. writing—review & editing; J. W. supervision; J. W. and J. J. funding acquisition.

Conflict of interest—The authors declare no competing interests.

Abbreviations—The abbreviations used are: CR, cell recovery; CSRP, cross-species razor protein; DMEM, Dulbecco's modified Eagle's medium; ECM, extracellular matrix; hc-MC, high-confidence Matrigel contaminant; LIR, low incorporation ratio; PCT, pressure cycling technology; PE, PBS-EDTA; pMC, potential Matrigel contaminant; SILAC, stable isotope labeling by amino acids in cell culture; ZIR, zero incorporation ratio.

Received June 30, 2021, and in revised form, October 25, 2021
Published, MCPRO Papers in Press, December 3, 2021, <https://doi.org/10.1016/j.mcpro.2021.100181>

REFERENCES

1. van de Wetering, M., Francies, H. E., Francis, J. M., Bounova, G., Iorio, F., Pronk, A., van Houdt, W., van Gorp, J., Taylor-Weiner, A., Kester, L., McLaren-Douglas, A., Blokker, J., Jaksani, S., Bartfeld, S., Volckman, R., *et al.* (2015) Prospective derivation of a living organoid biobank of colorectal cancer patients. *Cell* **161**, 933–945
2. Boj, S. F., Hwang, C. I., Baker, L. A., Chio, I. I., Engle, D. D., Corbo, V., Jager, M., Ponz-Sarvisé, M., Tiriac, H., Spector, M. S., Gracanin, A., Oni, T., Yu, K. H., van Boxtel, R., Huch, M., *et al.* (2015) Organoid models of human and mouse ductal pancreatic cancer. *Cell* **160**, 324–338
3. Lee, S. H., Hu, W., Matulay, J. T., Silva, M. V., Owczarek, T. B., Kim, K., Chua, C. W., Barlow, L. J., Kandoth, C., Williams, A. B., Bergren, S. K., Pietzak, E. J., Anderson, C. B., Benson, M. C., Coleman, J. A., *et al.* (2018) Tumor evolution and drug response in patient-derived organoid models of bladder cancer. *Cell* **173**, 515–528.e17
4. Drost, J., and Clevers, H. (2018) Organoids in cancer research. *Nat. Rev. Cancer* **18**, 407–418
5. Lau, H. C. H., Kranenburg, O., Xiao, H., and Yu, J. (2020) Organoid models of gastrointestinal cancers in basic and translational research. *Nat. Gastroenterol. Hepatol.* **17**, 203–222
6. Cristobal, A., van den Toorn, H. W. P., van de Wetering, M., Clevers, H., Heck, A. J. R., and Mohammed, S. (2017) Personalized proteome profiles of healthy and tumor human colon organoids reveal both individual diversity and basic features of colorectal cancer. *Cell Rep.* **18**, 263–274
7. Nascimento, J. M., Saia-Cereda, V. M., Sartore, R. C., da Costa, R. M., Schitine, C. S., Freitas, H. R., Murgu, M., de Melo Reis, R. A., Rehen, S. K., and Martins-de-Souza, D. (2019) Human cerebral organoids and fetal brain tissue share proteomic similarities. *Front. Cell Dev. Biol.* **7**, 303
8. Williams, K. E., Lemieux, G. A., Hassiss, M. E., Olshen, A. B., Fisher, S. J., and Werb, Z. (2016) Quantitative proteomic analyses of mammary organoids reveals distinct signatures after exposure to environmental chemicals. *Proc. Natl. Acad. Sci. U. S. A.* **113**, E1343–E1351
9. Padmanaban, V., Grasset, E. M., Neumann, N. M., Fraser, A. K., Henriët, E., Matsui, W., Tran, P. T., Cheung, K. J., Georgess, D., and Ewald, A. J. (2020) Organotypic culture assays for murine and human primary and metastatic-site tumors. *Nat. Protoc.* **15**, 2413–2442
10. Benton, G., Arnaoutova, I., George, J., Kleinman, H. K., and Koblinksi, J. (2014) Matrigel: From discovery and ECM mimicry to assays and models for cancer research. *Adv. Drug Deliv. Rev.* **79–80**, 3–18
11. Clevers, H. (2016) Modeling development and disease with organoids. *Cell* **165**, 1586–1597
12. Hughes, C. S., Postovit, L. M., and Lajoie, G. A. (2010) Matrigel: A complex protein mixture required for optimal growth of cell culture. *Proteomics* **10**, 1886–1890
13. Sampaziotis, F., de Brito, M. C., Geti, I., Bertero, A., Hannan, N. R., and Vallier, L. (2017) Directed differentiation of human induced pluripotent stem cells into functional cholangiocyte-like cells. *Nat. Protoc.* **12**, 814–827
14. Roper, J., Tammela, T., Akkad, A., Almqadadi, M., Santos, S. B., Jacks, T., and Yilmaz, Ö. H. (2018) Colonoscopy-based colorectal cancer modeling in mice with CRISPR-Cas9 genome editing and organoid transplantation. *Nat. Protoc.* **13**, 217–234
15. Kawasaki, K., Toshimitsu, K., Matano, M., Fujita, M., Fujii, M., Togasaki, K., Ebisudani, T., Shimokawa, M., Takano, A., Takahashi, S., Ohta, Y., Nanki, K., Igarashi, R., Ishimaru, K., Ishida, H., *et al.* (2020) An organoid biobank of neuroendocrine neoplasms enables genotype-phenotype mapping. *Cell* **183**, 1420–1435.e21
16. Dijkstra, K. K., Cattaneo, C. M., Weeber, F., Chalabi, M., van de Haar, J., Fanchi, L. F., Slagter, M., van der Velden, D. L., Kaing, S., Kelderman, S., van Rooij, N., van Leerdam, M. E., Depla, A., Smit, E. F., Hartemink, K. J., *et al.* (2018) Generation of tumor-reactive T cells by co-culture of peripheral blood lymphocytes and tumor organoids. *Cell* **174**, 1586–1598.e12
17. Driehuis, E., Kretzschmar, K., and Clevers, H. (2020) Establishment of patient-derived cancer organoids for drug-screening applications. *Nat. Protoc.* **15**, 3380–3409
18. Xiang, Y., Tanaka, Y., Patterson, B., Hwang, S.-M., Hysolli, E., Cakir, B., Kim, K.-Y., Wang, W., Kang, Y.-J., Clement, E. M., Zhong, M., Lee, S.-H., Cho, Y. S., Patra, P., Sullivan, G. J., *et al.* (2020) Dysregulation of BRD4 function underlies the functional abnormalities of MeCP2 mutant neurons. *Mol. Cell* **79**, 84–98.e9
19. Vlachogiannis, G., Hedayat, S., Vatsiou, A., Jamin, Y., Fernández-Mateos, J., Khan, K., Lampis, A., Eason, K., Huntingford, I., Burke, R., Rata, M., Koh, D.-M., Tunariu, N., Collins, D., Hulkki-Wilson, S., *et al.* (2018) Patient-derived organoids model treatment response of metastatic gastrointestinal cancers. *Science* **359**, 920–926
20. Lindeboom, R. G., van Voorthuisen, L., Oost, K. C., Rodríguez-Colman, M. J., Luna-Velez, M. V., Furlan, C., Baraille, F., Jansen, P. W., Ribeiro, A., Burgering, B. M., Snippert, H. J., and Vermeulen, M. (2018) Integrative multi-omics analysis of intestinal organoid differentiation. *Mol. Syst. Biol.* **14**, e8227
21. Tölle, R. C., Gaggioli, C., and Dengjel, J. (2018) Three-dimensional cell culture conditions affect the proteome of cancer-associated fibroblasts. *J. Proteome Res.* **17**, 2780–2789
22. Bartfeld, S., Bayram, T., van de Wetering, M., Huch, M., Begthel, H., Kujala, P., Vries, R., Peters, P. J., and Clevers, H. (2015) *In vitro* expansion of human gastric epithelial stem cells and their responses to bacterial infection. *Gastroenterology* **148**, 126–136.e6
23. Guo, T., Kouvonon, P., Koh, C. C., Gillet, L. C., Wolski, W. E., Röst, H. L., Rosenberger, G., Collins, B. C., Blum, L. C., Gillessen, S., Joerger, M., Jochum, W., and Aebersold, R. (2015) Rapid mass spectrometric conversion of tissue biopsy samples into permanent quantitative digital proteome maps. *Nat. Med.* **21**, 407–413
24. Cox, J., and Mann, M. (2008) MaxQuant enables high peptide identification rates, individualized p.p.b.-range mass accuracies and proteome-wide protein quantification. *Nat. Biotechnol.* **26**, 1367–1372
25. Aisenbrey, E. A., and Murphy, W. L. (2020) Synthetic alternatives to Matrigel. *Nat. Rev. Mater.* **5**, 539–551
26. Zhang, B., Wang, J., Wang, X., Zhu, J., Liu, Q., Shi, Z., Chambers, M. C., Zimmerman, L. J., Shaddock, K. F., Kim, S., Davies, S. R., Wang, S., Wang, P., Kinsinger, C. R., Rivers, R. C., *et al.* (2014) Proteogenomic characterization of human colon and rectal cancer. *Nature* **513**, 382–387
27. Jiang, Y., Sun, A., Zhao, Y., Ying, W., Sun, H., Yang, X., Xing, B., Sun, W., Ren, L., Hu, B., Li, C., Zhang, L., Qin, G., Zhang, M., Chen, N., *et al.* (2019) Proteomics identifies new therapeutic targets of early-stage hepatocellular carcinoma. *Nature* **567**, 257–261
28. Gillette, M. A., Satpathy, S., Cao, S., Dhanasekaran, S. M., Vasaikar, S. V., Krug, K., Petralia, F., Li, Y., Liang, W.-W., Reva, B., Krek, A., Ji, J., Song, X., Liu, W., Hong, R., *et al.* (2020) Proteogenomic characterization reveals therapeutic vulnerabilities in lung adenocarcinoma. *Cell* **182**, 200–225.e35
29. Sinha, A., Huang, V., Livingstone, J., Wang, J., Fox, N. S., Kurganovs, N., Ignatchenko, V., Fritsch, K., Donmez, N., Heisler, L. E., Shiah, Y.-J., Yao, C. Q., Alfaro, J. A., Volik, S., Lapuk, A., *et al.* (2019) The proteogenomic landscape of curable prostate cancer. *Cancer Cell* **35**, 414–427.e6
30. Schiller, H. B., Fernandez, I. E., Burgstaller, G., Schaab, C., Scheltema, R. A., Schwarzmayr, T., Strom, T. M., Eickelberg, O., and Mann, M. (2015)

- Time- and compartment-resolved proteome profiling of the extracellular niche in lung injury and repair. *Mol. Syst. Biol.* **11**, 819
31. Naba, A., Clauser, K. R., Hoersch, S., Liu, H., Carr, S. A., and Hynes, R. O. (2012) The matrisome: In silico definition and *in vivo* characterization by proteomics of normal and tumor extracellular matrices. *Mol. Cell. Proteomics* **11**. M111.014647
 32. Rao, S. S., Dejesus, J., Short, A. R., Otero, J. J., Sarkar, A., and Winter, J. O. (2013) Glioblastoma behaviors in three-dimensional collagen-hyaluronan composite hydrogels. *ACS Appl. Mater. Inter.* **5**, 9276–9284
 33. Gjorevski, N., Sachs, N., Manfrin, A., Giger, S., Bragina, M. E., Ordóñez-Morán, P., Clevers, H., and Lutolf, M. P. (2016) Designer matrices for intestinal stem cell and organoid culture. *Nature* **539**, 560–564
 34. Sachs, N., de Ligt, J., Kopper, O., Gogola, E., Bounova, G., Weeber, F., Balgobind, A. V., Wind, K., Gracanin, A., Begthel, H., Korving, J., van Boxtel, R., Duarte, A. A., Lelieveld, D., van Hoeck, A., *et al.* (2018) A living biobank of breast cancer organoids captures disease heterogeneity. *Cell* **172**, 373–386.e10
 35. Yan, H. H. N., Siu, H. C., Law, S., Ho, S. L., Yue, S. S. K., Tsui, W. Y., Chan, D., Chan, A. S., Ma, S., Lam, K. O., Bartfeld, S., Man, A. H. Y., Lee, B. C. H., Chan, A. S. Y., Wong, J. W. H., *et al.* (2018) A comprehensive human gastric cancer organoid biobank captures tumor subtype heterogeneity and enables therapeutic screening. *Cell Stem Cell* **23**, 882–897.e11
 36. Jacob, F., Salinas, R. D., Zhang, D. Y., Nguyen, P. T. T., Schnoll, J. G., Wong, S. Z. H., Thokala, R., Sheikh, S., Saxena, D., Prokop, S., Liu, D. A., Qian, X., Petrov, D., Lucas, T., Chen, H. I., *et al.* (2020) A patient-derived glioblastoma organoid model and biobank recapitulates inter- and intratumoral heterogeneity. *Cell* **180**, 188–204.e22